JOURNAL OF MATERIALS SCIENCE 6 (1971) 189-199

# The Effects of Alloying Material on Regrowth-layer Structure in Silicon Power Devices

F. M. ROBERTS, E. L. G. WILKINSON
*GEC - English Electric Co. Ltd, Nelson Research Laboratories, Beaconhill, Staffordshire, UK*

The effects on silicon regrowth-layer structure of pure aluminium are compared with those of aluminium-silicon alloy of eutectic composition when these are used as alloying material in joining silicon discs to metal contacts.

Non-uniform dissolution of silicon by pure aluminium is prevalent, and the configuration of the regrowth and undissolved silicon surfaces shows dissolution in preferred crystallographic directions. Measurements of recesses in the surfaces show that penetration into the silicon to depths of the order of 100 $\mu$m may occur during alloying. This is sufficient to penetrate diffused junctions resulting in the formation of local alloyed junctions of irregular shape with disastrous effects on the electrical characteristics of the device. Deep penetration is caused by a high solubility for silicon being suddenly presented locally when melting of the aluminium is initiated at points where conditions are most favourable.

In contrast aluminium-silicon eutectic alloy does not dissolve further silicon immediately on melting, and deep local penetration can thereby be avoided.

Measurements made on devices incorporating aluminium-silicon eutectic alloy show reductions in mean penetration depths of over 50%, and the elimination of those regrowth configurations that indicate dissolution in preferred directions.

## 1. Introduction

In the construction of high-power semiconductor p-n junction devices, the semiconductor component, usually a silicon slice containing diffused or epitaxially-grown layers, or both, is joined by an intermediate alloy foil disc to a metal contact support disc, of molybdenum, tungsten or sintered material. In the alloying process, during the temperature excursion experienced by the components assembled in a jig, the foil melts and dissolves part of the silicon slice. At the contact metal/melt interface some of the silicon in solution reacts with the contact material to form a metal silicide layer on the contact disc. This depletes the silicon content in the melt and leads to the solution of additional silicon from the slice, so that there is an equilibrium transport of silicon from the slice to the contact disc while the alloy is molten. On cooling, silicon rich in alloying metal is deposited from the melt onto the undissolved portion of the silicon slice, forming a regrowth-layer. This layer is in fact monocrystalline epitaxial material grown onto the remaining portion of the silicon slice by a liquid epitaxy process [1]. As the temperature falls further the whole of the remaining metal-silicon alloy solidifies, bonding the silicon and contact discs together. Fig. 1a illustrates a section of the final structure diagrammatically.

A proportion of devices produced in this or similar ways exhibit poor electrical characteristics after alloying and, although other factors may be involved, it is evident that these unsatisfactory results are often associated with the alloying process. It is therefore of interest to examine the process, and the materials used in it, in relation to the structure of the various layers in the resulting semiconductor/metal sandwich.

## 2. Experimental Method

### 2.1. General

A comparison of the effects on silicon regrowth-layer structure of pure aluminium with those of eutectic aluminium-silicon alloy used as alloying

© 1971 Chapman and Hall Ltd.

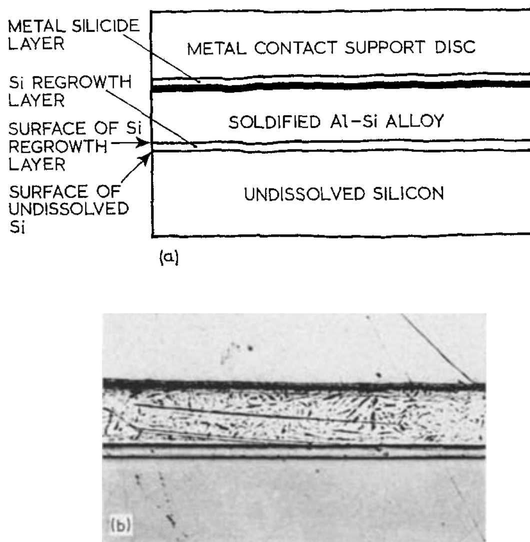


*Figure 1* Cross section of alloyed joint between silicon and metal.

material in joining silicon discs to metal contacts was made. The alloying material was in the form of foil discs, and both tungsten and molybdenum contacts were employed. The alloying thermal cycles took place in RF-heated vacuum furnaces and in inert gas atmosphere resistance-heated furnaces, the components being assembled in powder-filled or solid graphite jigs. The surfaces of the silicon discs used coincided with (111) planes within the usual tolerances The diameters of the regrowth-layers examined were 12.5 mm and 25 mm. The maximum temperatures to which the assemblies were raised ranged from 700 to 880° C.

### 2.2. Examination of Specimens

The structure of the silicon regrowth-layers in specimens prepared by the method described above was examined. In order to gain access to and examine the whole area of the surface of the regrowth-layer, it was necessary to separate the components of the sandwich silicon/alloy/metal without damaging the regrowth-layer (see fig. 1b). By chemical removal of the solidified aluminium-silicon alloy layer, the silicon and metal discs were separated without damaging either, and both the silicon regrowth-layer surface and that of the metal silicide layer were made available for inspection. Dissolution of the aluminium-silicon alloy layer was achieved by a variety of techniques, the simplest, though the most time consuming, of which [2] is to immerse the sandwiches in hydrochloric acid for several days.

The silicon regrowth-layer was removed by a selective etchant (1:3:10 $HF$:$HNO_3$:$CH_3COOH$), revealing the surface of the undissolved silicon, i.e. the solid side of the interface between the silicon and the molten alloy at the maximum depth of penetration reached during the thermal cycle.

Measurement of features in the surface of the layers was made under the microscope by differential focusing. Regrowth-layer thicknesses were also measured in angle-lapped sections by differential focusing and interferometry.

## 3. Experimental Results

### 3.1. Visual Examination of Silicon Regrowth-Layer Surface

Examination of the silicon regrowth-layer surface revealed features common to all specimens. In no case was this surface perfectly plane. Recesses or undulations were present in every sample examined. However, there were differences in surface configuration between samples in which pure aluminium alloying material had been used and those incorporating aluminium-silicon alloy.

#### *3.1.1. Pure Aluminium*

Samples of tungsten/aluminium/silicon sandwiches fired in argon in resistance-heated furnaces, to maximum temperatures of between 700 and 800° C, and which had exhibited poor electrical characteristics, revealed, in every case, well-defined recesses in the regrowth-layer surfaces. In some cases these were few and individually large in area; in others there were many small recesses (fig. 2). The density of recesses was sometimes fairly uniform over the whole surface; in other cases recesses were unevenly distributed and there were adjacent areas of high and low recess density. Although recesses assumed a variety of shapes, the most common was that of a letter Y or three-pointed star, together with dendritic variations of this shape, with trunks and branches at approximately 120° (see fig. 3). Shapes intermediate between the Y-star and equilateral triangles were also common.

Recesses sufficiently near the edge of the silicon disc were visible before separation of the components, having been revealed by the edge bevelling process commonly used in high-voltage devices as a method of surface field control (fig. 4).

### *3.1.2. Aluminium-Silicon Alloy*

Specimens of molybdenum/aluminium-silicon/silicon/silver-lead-antimony/molybdenum sandwiches fired in vacuum at temperatures approximating to 830° C were examined similarly. The surfaces of the silicon regrowth-layer in these samples was undulatory, and recesses were irregular in shape with ill-defined edges. No Y-star or triangular shapes were found (fig. 5).

A third series of regrowth surfaces examined was from sandwiches of molybdenum/aluminium-silicon/silicon/gold-antimony fired in vacuum to temperatures in the range 700 to 750° C. In this series the furnace and jigging arrangements were such that during the whole thermal cycle the aluminium-silicon remained at a higher temperature than the silicon, so that a decreasing positive temperature gradient [3] from melt to solid silicon was maintained. In these specimens the silicon regrowth-layer surfaces were also un-

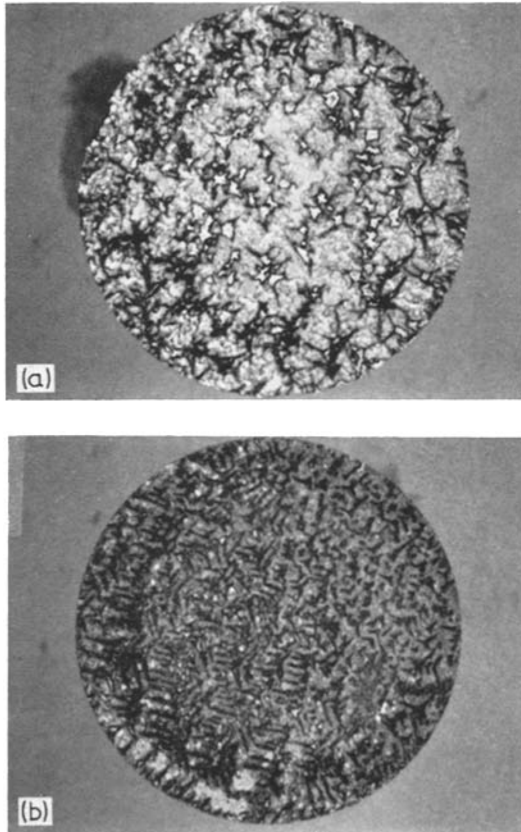


*Figure 2* Recesses in silicon regrowth-layer surfaces. (a) Small number of non-uniformly distributed large recesses. Specimen 30 (× 5.5). (b) Large number of smaller recesses. Specimen 31 (× 5.5).

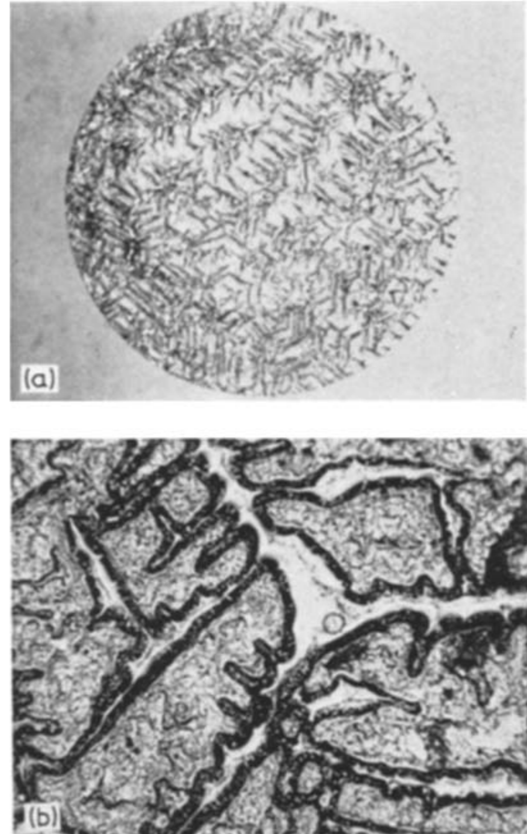


*Figure 3* Y-shaped recesses in surfaces of silicon regrowth-layers using pure aluminium. (a) Specimen 12 (× 5.5). (b) Specimen 13 (× 50).

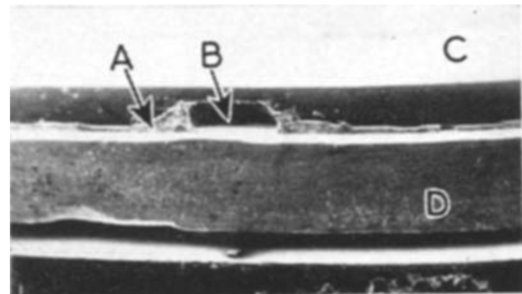


*Figure 4* Deep penetration of aluminium into silicon revealed by bevelling. Specimen 7. Scanning electron micrograph (× 12).
A = Aluminium, B = Recess, C = Silicon slice, D = Metal contact support disc.

dulatory, but the surface features were less pronounced than in the previous series (fig. 6).

### *3.1.3. Measurement of Recess Depths*

Representative samples of the deeper recesses in

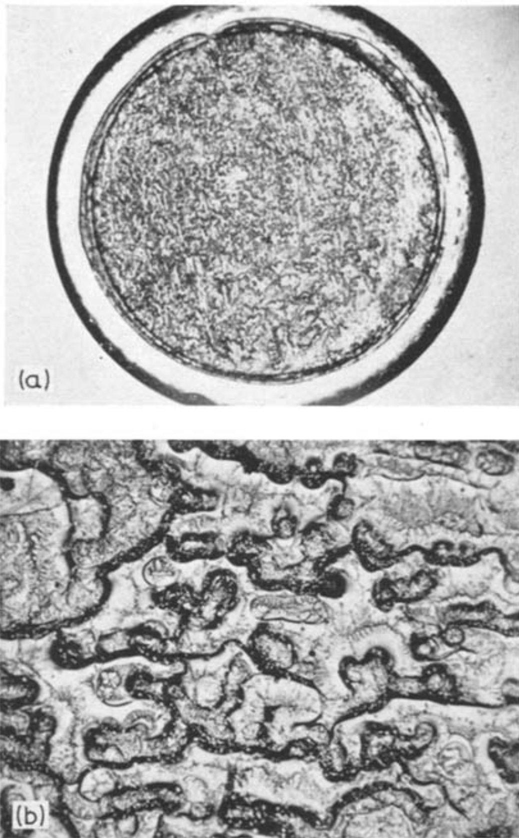

*Figure 5* Surface of silicon regrowth-layer using aluminium silicon alloy. (a) Specimen B136.89 cc (× 4.6). (b) Specimen B136.89 cc (× 50).

the silicon regrowth-layer surfaces in each specimen were measured. Results from typical specimens of the three types described above are shown in fig. 7. Both mean and maximum recess-depths are less in samples with aluminium-silicon alloy than in those containing pure aluminium, and in the former the effect of a favourable temperature gradient is to reduce the mean, if not always the maximum, depth. (The area of the regrowth-layer surface in the "temperature gradient" series was four times larger than in the other series.)

Specimens in the three series examined so far originated from devices of a variety of types, fired in different furnaces in various jig designs. In order further to compare the effects of aluminium with those of aluminium-silicon alloy in similar assemblies alloyed in as far as possible identical firing and jigging conditions, a fourth series of silicon/alloying foil/metal sandwiches were alloyed in graphite powder jigs, some individually and others stacked more than one per jig, in an argon atmosphere in a resistance-heated furnace. The jig arrangements are shown in fig. 8.

Representative results of measurements of depths of recesses in the regrowth-layer surfaces are compared in table I and fig. 9. Both mean and maximum recess depths were smaller in samples containing aluminium-silicon alloy than in those incorporating pure aluminium. The material of the contact disc did not affect the depths of the recesses.

### *3.1.4. Effects of Temperature Gradient*

Some sets of components in the fourth series were assembled, silicon upwards (positive), others metal upwards (negative), in the single device jigs. The thermal path to one face of the components was rendered longer than to the other by loading a quantity of graphite powder, of

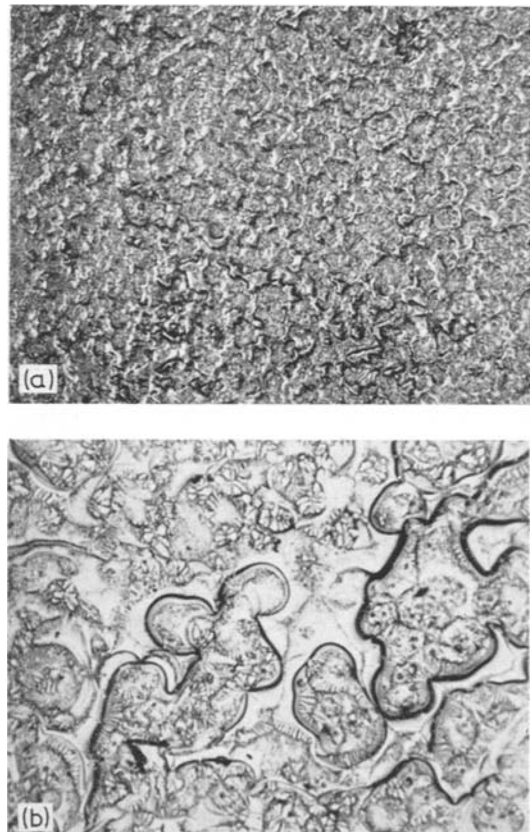

*Figure 6* Devices with 25 mm diameter Si/Al-Si/Mo joint fired in a favourable temperature gradient. Surface of silicon regrowth-layer. (a) Specimen TG83 (× 10). (b) Specimen TG84 (× 50).

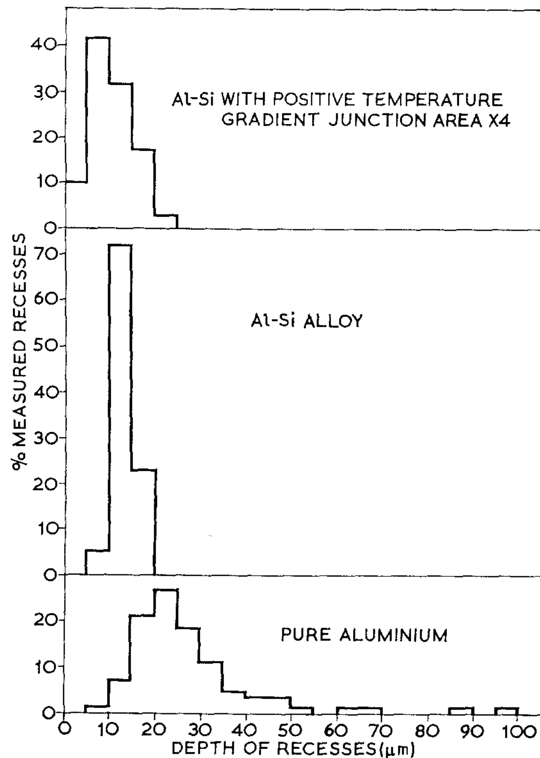


*Figure 7* Comparison of distribution of depths of recesses in the surfaces of silicon regrowth-layers (series 1-3 devices).

comparatively low thermal conductivity, above the assembled components [3]. This arrangement tends to set up a thermal gradient across the components during heating. In these experiments this gradient was not measured, and no special precautions were taken in the method of heating to induce such a gradient. However the results (table II) indicate a slight decrease in mean, and a considerable reduction in maximum depth of recesses, when the silicon was assembled adjacent to the powder, and is therefore likely to have been cooler than the melt during heating.

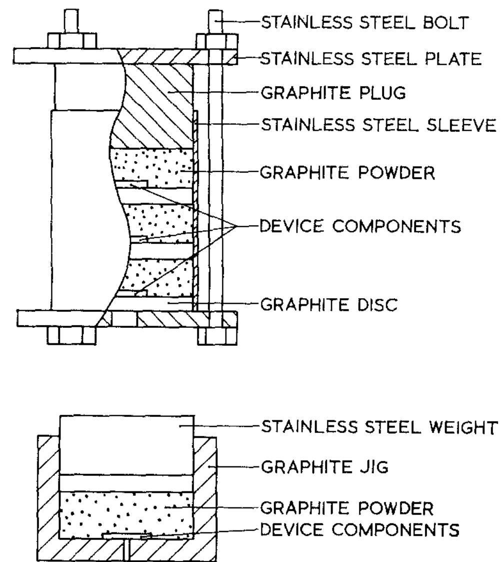


*Figure 8* Series 4 jig arrangements.

### 3.2. Visual Examination of Undissolved Silicon Surface

Comparison of micrographs of specimens incorporating pure aluminium before and after removal of the regrowth-layer shows that recesses in the undissolved silicon surface correspond in shape to those above them in the surface of the regrowth-layer (fig. 10).

The distribution of depths of recesses in the regrowth-layer surfaces is compared with that of depths in the undissolved silicon surfaces in specimens 30 and 31 (fig. 11). In each the mean depths are greater in the undissolved silicon surface than in the regrowth-layer surface. A typical variation of regrowth-layer thickness is shown in fig. 12, in which a silicon disc, after removal of aluminium-silicon alloy, has been angle-lapped and etched to reveal the regrowth-layer section on the lapped surface. The regrowth-layer, flat-based under the base of the

TABLE I Effect of foil material on depths of recesses in the fourth series of devices. Process depth μm.

| | | Al P3-P7 | Al-Si P10-P13 | Al P8 & P9 | Al-Si P17 & P19 | Al P21 & P13 | Al-Si P20 & P22 |
|---|---|---|---|---|---|---|---|
| Regrowth-surface | Max | 47 | 32 | 40 | 17 | 64 | 2 |
| | Mean | 24 | 13 | 21 | 9 | 36 | 12 |
| Undissolved silicon | Max | 90 | 45 | 40 | 17 | 77 | 29 |
| | Mean | 43.6 | 21.7 | 25.5 | 10.3 | 42.5 | 15.2 |

Note: the specimen numbers refer to Different JIG arrangements.

TABLE II Temperature gradient effect on depths of recesses in the fourth series of devices. Process depth $\mu$m.

| | | Aluminium P4 & P6 (+ ve) | P5 & P7 (− ve) | Aluminium Silicon P10 & P12 (+ ve) | P11 & P13 (− ve) |
|---|---|---|---|---|---|
| Regrowth-surface | Max | 37 | 47 | 24 | 32 |
| | Mean | 22.7 | 25.8 | 12.05 | 13.48 |
| Undissolved silicon | Max | 74 | 90 | 24 | 45 |
| | Mean | 39.6 | 47.6 | 16.9 | 26.4 |

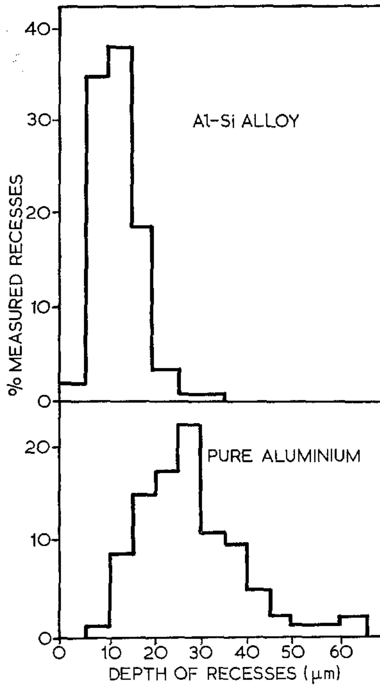


*Figure 9* Distribution of depths of recesses in silicon regrowth-layer surfaces in series 4 devices.

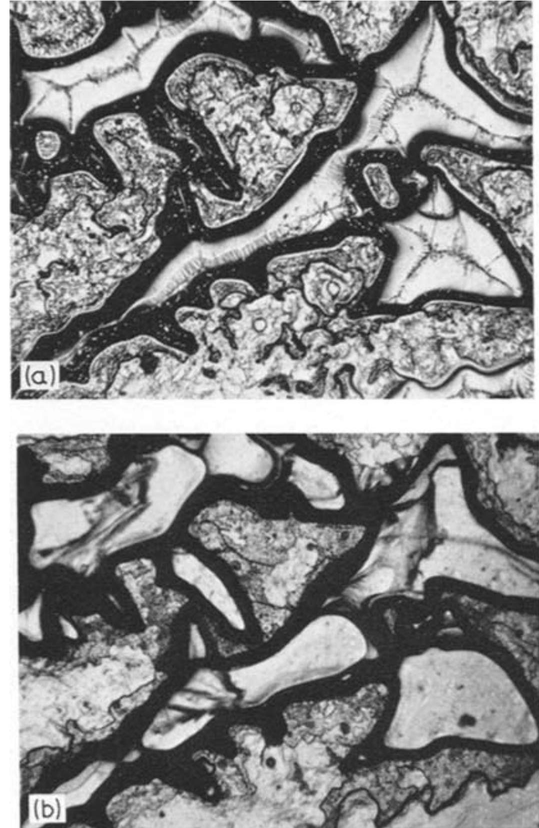


*Figure 10* Surfaces of silicon regrowth-layer and undissolved silicon. Specimen 38. (a) Recess in surface of silicon regrowth-layer after removal of aluminium silicon alloy (× 62). (*b*) Corresponding recess in surface of undissolved silicon after removal of regrowth-layer.

recess in the surface, is seen to be thicker there than it is near the edge of the recess.

The distribution of depths of recesses in the surface of the undissolved silicon layer in the final series of specimens is shown in table I.

## 4. Discussion

### 4.1. Effects of Non-uniform Alloying

Visual examination and measurement of recesses in regrowth-layer and undissolved-silicon surfaces in specimens incorporating pure aluminium as alloying material, show that depths of attack into silicon during the alloying process are sufficient in some cases to penetrate diffused junctions, which in power devices are often from 50 to 75 $\mu$m below the silicon surface, or through epitaxial layers of similar thickness or less. On solidification alloyed p-n junctions of irregular shape are formed in regions where penetration has taken place, with disastrous results on the electrical characteristics of the device.

### 4.2. Initiation of Melting

Consideration of the aluminium-silicon equilibrium phase diagram in relation to the components used and the jigging and firing conditions indicates the cause of the irregular interfaces and

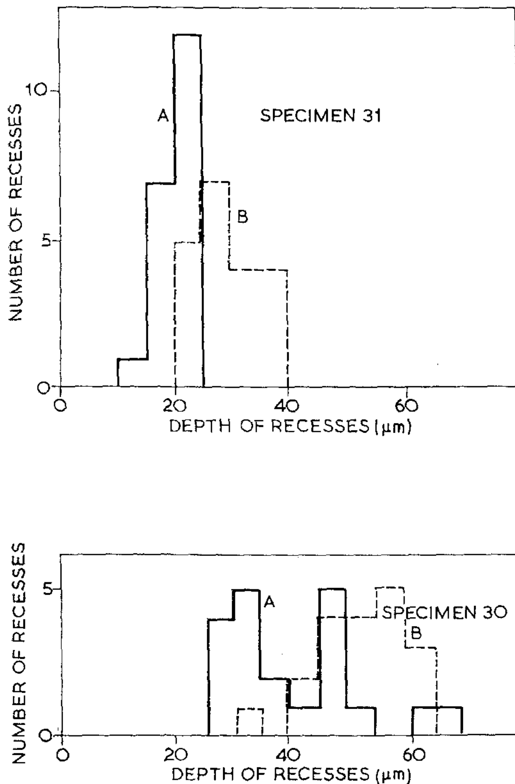


*Figure 11* Distribution of depths of recesses in surfaces of silicon regrowth-layers (A) and undissolved silicon (B) in specimens 30 and 31 employing pure aluminium.

the locally deep penetration. Considering first pure aluminium, as the temperature rises during the alloying thermal cycle, no melting occurs until the temperature of the components rises well above the aluminium-silicon eutectic melting point of 577° C to, or very close to, the melting point of aluminium (660° C), since no material of eutectic composition is initially present (fig. 14).

Conditions for the initiation of solution of silicon into the aluminium vary in favourability at different points on the silicon surface. Dislocation density, for instance, may be greater near the edge than at the centre of the slice. Because of the strain energy associated with a dislocation, removal of silcon atoms from the lattice requires least energy at positions where dislocations emerge at the surface, and among these, at those dislocations with the largest Burgers vectors.

Because none of the components of the assembly have perfectly flat surfaces, pressure at the aluminium/silicon interface is greater at some points than at others. Thermal conduction across the faces at these points is greater than elsewhere, so that incoming thermal energy raises the temperatures of zones around these points to higher levels than at other interface areas where contact is not so intimate. These zones of highest pressure and best contact therefore approach the melting point in advance of less-favoured areas. Diffusion of aluminium into silicon is thus initiated and liquid nuclei appear [4, 5].

Other factors such as thickness and continuity of oxide films on surfaces in contact may affect the initiation of melting. Dissolution of the silicon therefore begins at points where the optimum value of all such factors coincide, and not uniformly over the whole surface of the silicon disc.

### 4.3. Directionally Preferential Dissolution

When the aluminium at and around such initiation points melts there becomes immediately available a large capacity for dissolving silicon. Silicon solubility in aluminium at the percentage appropriate to the temperature of the compo-

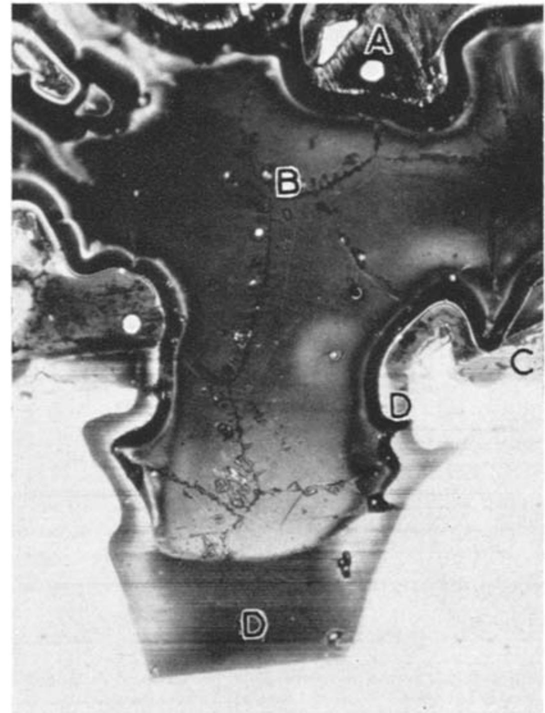


*Figure 12* Angle-lapped section showing flat base of regrowth-layer under recess in regrowth surface. Specimen 16 (× 125). A = Surface of regrowth-layer, B = Recess, C = Edge of bevel, D = Regrowth-layer.

nents at that time, i.e. about 660° C, is shown on the phase diagram (fig. 14) by the composition corresponding to that temperature on the silicon-rich side of the liquidus line, to be approximately 16 to 17 at. % of silicon [6]. Silicon atoms are therefore removed from the lattice and taken into solution until the proportion of silicon in the melt reaches this percentage. Since the system does not reach equilibrium until this melt composition is achieved, silicon atoms are removed from the lattice at a fast rate, dissolution proceeding in directions where lie atoms that require the least expenditure of energy to break the bands joining them to the lattice. In other words, the most loosely-bonded atoms are removed preferentially. Dissolution therefore proceeds in preferred crystallographic directions.

Single crystal growth in group IV elements has been shown [7] to take place in the [111] direction by the lateral flow of unit steps of ⟨110⟩ chains of atoms in (111) planes in the ⟨112⟩ directions normal to these chains. Growth in the $[\bar{1}\bar{1}2]$ directions occurs preferentially to that in the $[11\bar{2}]$ direction, since two free bonds are available for the attachment of the incoming atom in the former case, whereas only one is available in the latter. By a reversal of this process [8], dissolution in the $[11\bar{2}]$ direction is preferred, since this requires the breaking of fewer bonds per atom removed.

In the present case of non-equilibrium conditions dissolution of a silicon surface approximating to a (111) plane is therefore likely to take place preferentially in the $[11\bar{2}]$ direction. Penetration into the bulk of the silicon also proceeds in ⟨112⟩ directions in those (111) planes not parallel to the surface.

In (111) planes in the silicon lattice the ratio of the distances between adjacent atoms in ⟨112⟩ and ⟨110⟩ directions respectively is $\sqrt{3}$:1. If by the expenditure of a given amount of energy an equal number of atoms is removed in the $[11\bar{2}]$ direction and along a [110] chain, dissolution will have proceeded further in the $[11\bar{2}]$ than in the [110] direction. Dissolution of silicon preferentially along ⟨112⟩ directions from an initiation point thus produces Y-shaped figures with branches at angles of 120° to each other; in fact precisely such figures as have been observed in many of the surfaces of regrowth-layers and undissolved silicon in the specimens examined. Examples of the latter are shown in fig. 13. The process is illustrated diagrammatically, and related to the phase diagram, in fig. 14.

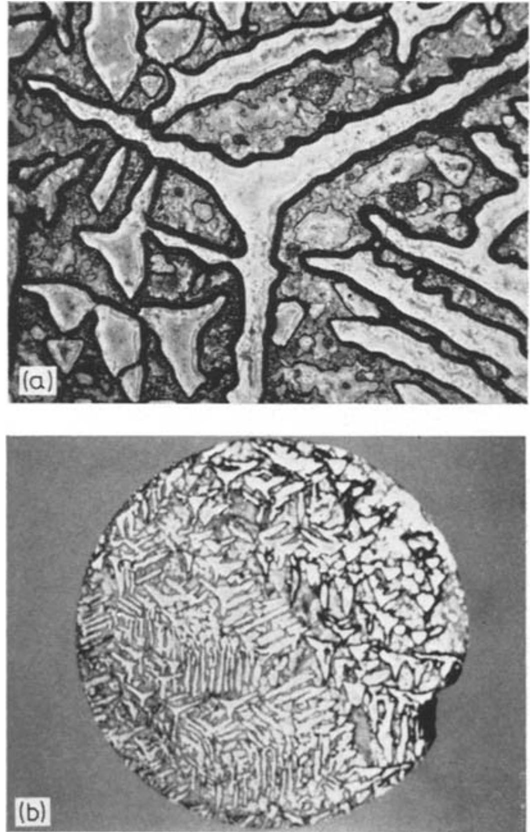


*Figure 13* Y-shaped recesses in surface of undissolved silicon. (a) Specimen 31 (× 50). (b) Specimen 21 (× 5.5).

Once the melt composition appropriate to the temperature is reached, further dissolution takes place in near-equilibrium conditions, and silicon is dissolved from areas of the disc surface between the zones of initial attack. However, less silicon is removed in these areas than would have been if the initial attack had been distributed uniformly over the surface.

### 4.4. Avoidance of Local Penetration

Local penetration is thus a consequence of fast removal of silicon atoms preferentially in ⟨112⟩ directions in order immediately to satisfy a suddenly-presented silicon solubility. Such penetration can therefore be reduced in depth by reducing the silicon solubility available at the initiation of melting. This reduction is achieved by the use of aluminium-silicon of eutectic composition instead of pure aluminium. Alloy of this composition melts at 577° C, and at this temperature no further silicon is taken into solution since the proportion of silicon appropri-

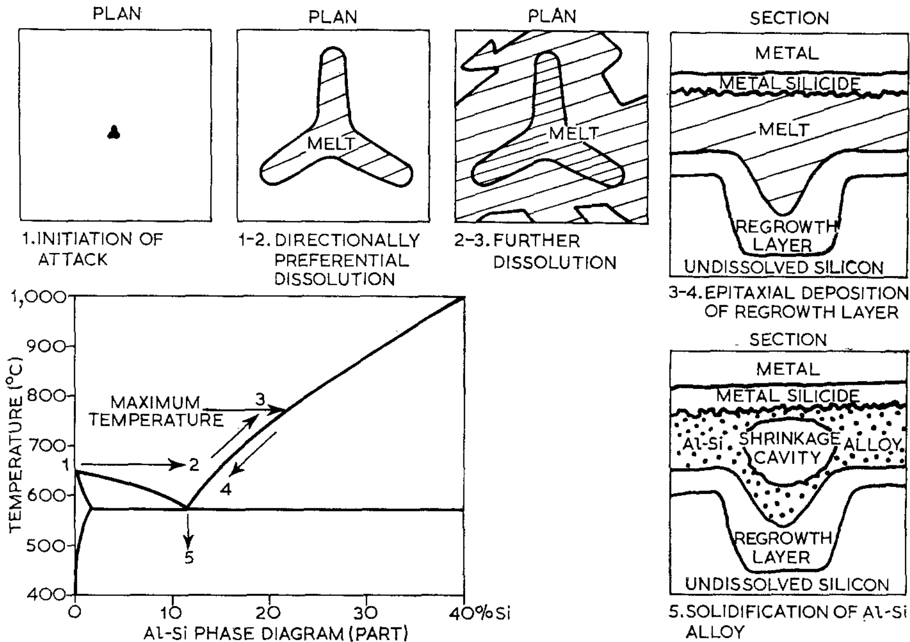


*Figure 14* Stages in the process of alloying silicon and metal discs together with pure aluminium.

ate to the temperature is already present in the alloying material. As the temperature rises and as silicon is withdrawn from the melt at the metal/melt interface to form metal silicide, further silicon is taken into solution from the surface of the silicon slice to maintain saturation. Dissolution of silicon thus begins in near-equilibrium conditions and there is little tendency towards directionally preferential attack.

If adverse temperature gradients are absent, crystallographic effects tend to limit penetration: the denser packing of atoms in (1 1 1) planes compared with that in other planes promotes dissolution across (1 1 1) surfaces. Shallow recesses approximating in shape to the frustum of a regular tetrahedron are formed and these spread laterally, joining or overlapping to form a comparatively plane surface. Control over the planarity of this melt/silicon interface is increased by imposing a positive temperature gradient across it, in which the melt is hotter than the silicon. This reinforces the crystallographic tendency towards planarity. The alloying process when a foil disc of aluminium-silicon alloy is included in the assembly is illustrated and related to the phase diagram in fig. 15.

### 4.5. Depth of Penetration in Relation to the Number of Points of Attack

In a series of similar devices incorporating pure aluminium the amount of silicon taken into solution immediately after the initiation of melting is virtually the same for each device, since the amount of aluminium is constant from device to device within practical limits. The energy available for dissolution depends on the temperature at the time melting starts, which is also virtually invariant when jig and furnace conditions remain the same. The depth of maximum penetration in any one specimen is therefore related to the number of points at which the silicon is attacked. Attack at a few points produces deeper local penetration than attack at many points, since the same total amount of silicon has to be removed from fewer sites. This is illustrated in fig. 2 and by the measurements of penetration depths in specimens 30 and 31 (fig. 11).

Aluminium-silicon alloy is advantageous in this respect also. At the initiation of melting at 577 °C no local penetration into the silicon takes place, and all the aluminium-silicon foil becomes molten virtually simultaneously. Pressure is then hydrostatically distributed over the whole area of the silicon, and thermal conductivity across the silicon/melt interface is therefore substantially uniform over the whole area of the silicon. The points at which dissolution actually begins are in these circumstances solely determined by the presence and relative magnitude of lattice defects at the surface.

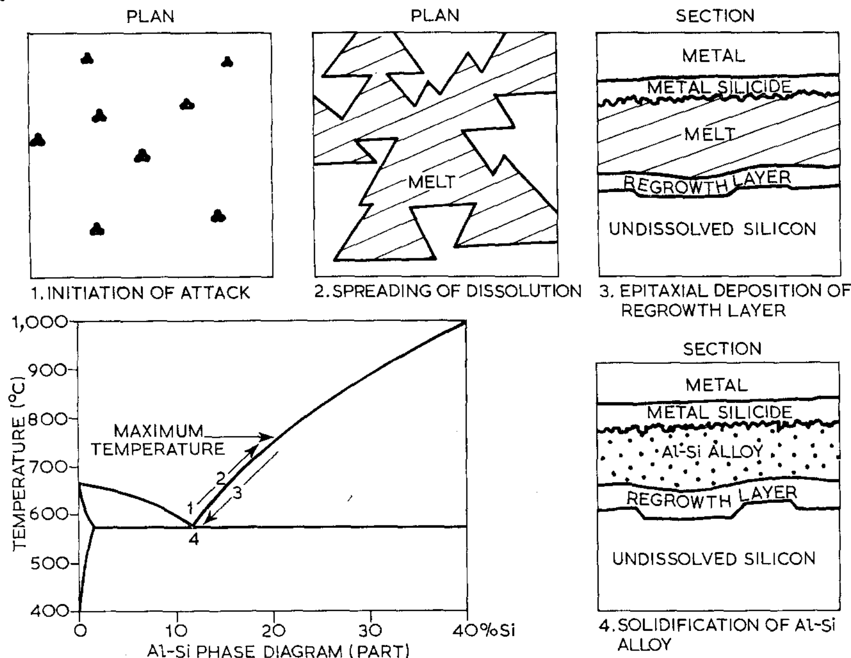


*Figure 15* Stages in the process of alloying silicon and metal discs together with aluminium-silicon.

### 4.6. Heating Rate in Relation to Uniformity of Alloying

It has been stated [3] that fast heating of semiconductor device assemblies promotes even melting and uniform alloying. This is true under certain conditions, but not necessarily true under all. Since the thermal conductivity of the assembly of jig and components is invariably anisotropic, thermally conductive paths from different points on the external surface of the jig to the critical interfaces of the components vary in thermal resistance. Fast heating is therefore likely to induce temperature gradients across the interfaces between components. The greater the thermal flow rate, the steeper these gradients will be. Unless the method of heating is chosen, and the jigs designed, to induce thermal flow in the desired direction, experience shows that frequently an adverse temperature gradient is produced. The faster the rate of heating, the worse will be the effect of the increasingly adverse temperature gradient and the less uniform will be the alloying. In situations where the method of firing is such that a desirable temperature gradient is difficult to achieve, it is preferable to aim to avoid all temperature gradients and rely on crystallographic effects (i.e. the (1 1 1) plane) and alloying material (i.e. material of semiconductor-metal eutectic composition) to promote uniform alloying. In order to minimise temperature gradients through the assembled components, slow heating rates are desirable in such circumstances.

## 5. Conclusions

Non-uniform dissolution of silicon occurs during alloying of p-n junction devices with pure aluminium by the fast removal of silicon preferentially in ⟨1 1 2⟩ directions in order to satisfy the solubility for silicon that suddenly arises at discrete points as the aluminium starts melting. Immediate improvement in uniformity of alloying is gained by substituting aluminium-silicon alloy for pure aluminium and reductions in mean penetration depth of over 50% have been achieved thus. Further improvement can be obtained by promoting a favourable temperature gradient through the components during the alloying thermal cycle.


## Acknowledgements

The authors thank Dr E. Eastwood, Director of Research, The General Electric and English Electric Companies Limited, for permission to publish this article.

## References


1. T. MITSUHATA, *Jap. J. Appl. Phys.* **9** (1970) 90.
2. C. G. BECK *et al*, *Electrochem. Tech.* **5** (1967) 377.
3. F. M. ROBERTS and E. L. G. WILKINSON, *J. Mater. Sci.* **3** (1968) 110.
4. YU. L. KRASILIN *et al*, *Neorganicheskie Materiali* **1** (1965) 1090.
5. V. D. TABELEV and A. A. ROSSOSHINSKII, *Welding Production* **15** (1968) 90.
6. W. GERLACH and B. GOEL, *Solid State Electron* **10** (1967) 589.
7. R. G. RHODES, "Imperfections and active centres in semiconductors" (Pergamon Press 1965) p. 170.
8. *Ibid*, p. 336.


Received 22 September and accepted 26 November 1970.